Floquet Topological Phase of Nondriven p-Wave Nonequilibrium Excitonic Insulators

E. Perfetto[1,2] and G. Stefanucci[1,2]

[1]Dipartimento di Fisica, Università di Roma Tor Vergata, Via della Ricerca Scientifica 1, 00133 Rome, Italy
[2]INFN, Sezione di Roma Tor Vergata, Via della Ricerca Scientifica 1, 00133 Rome, Italy

(Received 23 January 2020; accepted 14 August 2020; published 1 September 2020)

The nontrivial topology of p-wave superfluids makes these systems attractive candidates in information technology. In this work we report on the topological state of a p-wave nonequilibrium excitonic insulator (NEQ-EI) and show how to steer a nontopological band insulator with bright p excitons toward this state by a suitable laser pulse, thus achieving a dynamical topological phase transition. The underlying mechanism behind the transition is the broken gauge-symmetry of the NEQ-EI which causes self-sustained persistent oscillations of the excitonic condensate and hence a Floquet topological state for high enough exciton densities. We show the formation of Floquet Majorana modes at the boundaries of the open system and discuss unique topological spectral signatures for time-resolved ARPES experiments. We emphasize that the topological properties of a p-wave NEQ-EI arise exclusively from the electron-hole Coulomb interaction as the system is not driven by external fields.

DOI: 10.1103/PhysRevLett.125.106401

A quantum system with nontrivial bulk topological properties admits localized single-particle states at the system edges [1–3]. Existence of well-defined *quasiparticles* is of course a prerequisite for the bulk-edge correspondence to have physical relevance. In fact, most topological invariants are constructed from a quasiparticle Hamiltonian which is treated either as "noninteracting," i.e., independent of the charge distribution, or at a "mean-field" level. Mean-field Hamiltonians introduce an appealing twist in the topological characterization since, at fixed external potentials, they depend on the (self-consistent) charge distribution of the stationary state. Thus, in principle, a quantum system can change its topological properties upon a transition from an excited state to another. Furthermore, the possibility of self-sustained, i.e., not driven by external fields [4], oscillatory solutions extends the class of topological invariants to the Floquet realm [5–8].

Nonequilibrium (NEQ) excitonic insulators (EI) are excited states of band-insulator (BI) mean-field Hamiltonians giving rise to a self-sustained oscillating order parameter, i.e., the excitonic condensate (EC) [9–19]. In this Letter we show that a p-wave NEQ-EI undergoes a topological transition with increasing the EC density, leading to the formation of Floquet Majorana edge modes [20]. We further demonstrate that the Floquet topological p-wave NEQ-EI can be built up in real time by laser pulses of finite duration provided that p excitons exist and are optically active. As the initial BI ground state has vanishing EC density and trivial topology, the system experiences a *dynamical* phase transition (from BI to nontopological NEQ-EI) followed by a topological one. The density of topological defects predicted by the Kibble-Zurek mechanism [21,22] for external drivings of finite duration [23–28] can indeed be made sufficiently small to preserve the topological character of the final state. Unique spectral signatures for time-resolved ARPES investigations are also discussed. In particular, the spectral weight of the excitonic sideband experiences a "blockade" just before the topological transition, and at the transition the spectrum becomes gapless—the p-wave NEQ-EI turns into a Dirac semimetal.

Nonvanishing topological invariants [1,3] and existence of Majorana edge modes [29] in quantum matter with a p-wave symmetry-broken ground state have been recently reported for superconductors [30–33], superfluids of ultracold atomic gases [34], nanowires [35], insulators [2], and excitonic insulators [36–38]. In nonequilibrium and nondriven conditions, however, a nontrivial topology has so far been found only in the mean-field Floquet Hamiltonian of a p-wave superfluid [39].

The simplest description of a NEQ-EI is provided by a spinless one-dimensional Hamiltonian with a single valence and conduction bands separated by a direct gap of magnitude ϵ_g [19]:

$$\hat{H} = \sum_{\alpha j} (-)^{\alpha} [V \hat{\psi}^{\dagger}_{\alpha j} \hat{\psi}_{\alpha j+1} - (2V + \epsilon_g/2) \hat{n}_{\alpha j}] + \sum_{ij} U_{ij} \hat{n}_{vi} \hat{n}_{cj}, \tag{1}$$

where $\hat{\psi}_{vj}$ ($\hat{\psi}_{cj}$) annihilates a valence (conduction) electron in the jth cell, $\hat{n}_{\alpha j} \equiv \hat{\psi}^{\dagger}_{\alpha j} \hat{\psi}_{\alpha j}$ and $(-)^{\alpha} = 1, -1$ for $\alpha = v, c$ (the hopping integral V is chosen positive). The Hamiltonian is invariant under the "local" gauge

symmetry $\hat{\psi}_{\alpha j} \to e^{i\theta_\alpha}\hat{\psi}_{\alpha j}$ associated to the commutation relation $[\hat{H}, \hat{N}_\alpha] = 0$, with $\hat{N}_\alpha = \sum_j \hat{n}_{\alpha j}$. For large enough U_{ij} the ground state is a BI with a filled (empty) valence (conduction) band. Charge neutral excited states with $N_c = 1$ can be calculated by solving the Bethe-Salpeter equation (BSE). For short-range interactions, e.g., $U_{ij} = \delta_{ij}U$, the BSE admits only one discrete solution corresponding to an s-wave (even) exciton [19]. A Rydberg-like series, and hence p-wave (odd) excitons, appears with long-range interactions such as the soft-Coulomb one: $U_{ij} = U/\sqrt{|i-j|^2+1}$. Henceforth we express all energies in units of ϵ_g and choose $U = 2V = 1$. Then, the BSE admits multiple excitonic solutions, the two lowest having energy $\epsilon_x^s = 0.40$ (s wave) and $\epsilon_x^p = 0.82$ (p wave) above the valence band maximum. Charge-neutral excited states with a finite density in the conduction band will be treated in the mean-field approximation.

The lowest-energy excited state of $\hat{H}$ with a finite density of conduction electrons and valence holes equals the ground state of the NEQ gran-canonical Hamiltonian $\hat{H}_{\text{NEQ-GC}} \equiv \hat{H} - \mu_v\hat{N}_v - \mu_c\hat{N}_c$, where μ_α is the chemical potential for electrons in band α. Charge neutrality is guaranteed by $\mu_v = -\mu_c = -\delta\mu/2$ since $\hat{H}$ is particle-hole symmetric (the BI ground state is recovered for $\delta\mu = 0$). Exploiting the translational invariance, the mean-field equations for $\hat{H}_{\text{NEQ-GC}}$ can be written as [40]

$$\begin{pmatrix} -\epsilon_k + \delta\mu/2 & \Delta_k \\ \Delta_k & \epsilon_k - \delta\mu/2 \end{pmatrix} \begin{pmatrix} \varphi^\xi_{vk} \\ \varphi^\xi_{ck} \end{pmatrix} = \xi e_k \begin{pmatrix} \varphi^\xi_{vk} \\ \varphi^\xi_{ck} \end{pmatrix}, \quad (2)$$

where $\epsilon_k = \{2V[1-\cos(k)] + \epsilon_g/2\}$, $k \in (-\pi, \pi)$ is the quasimomentum, $\xi = \pm$ labels the two eigensolutions and $\Delta_k = -\sum_q \tilde{U}_{k-q} b_q$ is the excitonic order parameter, $\tilde{U}_k$ being the Fourier transform of U_{ij} and $b_q \equiv \varphi^-_{cq}\varphi^{-*}_{vq}$ the EC density. Only states of the minus branch are occupied since $e_k = \sqrt{(\epsilon_k - \delta\mu/2)^2 + \Delta_k^2} \geq 0$. Equation (2) has to be solved self-consistently and $\Delta_k \neq 0$ implies a symmetry-broken NEQ-EI state. Like ground-state EI's [41], no off-diagonal long-range order is present in NEQ-EI's. The system remains a BI ($\Delta_k = 0$) for $\delta\mu < \epsilon_x^s$, as it should be [16,19]. A unique solution $\Delta_k = \Delta_{-k}$ (even in k) exists for $\epsilon_x^s < \delta\mu < \epsilon_x^p$ (s-wave NEQ-EI). For $\delta\mu > \epsilon_x^p$ we can find a solution $\Delta_k = \Delta_k^s + \Delta_k^p$ with Δ_k^s (Δ_k^p) even (odd) in k for any fixed angle $\theta = \arctan(\Delta_\pi^s/\Delta_\pi^p) \in (0, 2\pi)$. The p-wave NEQ-EI state is realized when $\theta = 0$ and hence $\Delta_k = -\Delta_{-k}$. Below we show that this state can be generated by suitable laser pulses provided that the p-wave (s-wave) exciton is bright (dark).

Independently of the symmetry the NEQ-EI state evolves according to the time-dependent mean-field equations $i(d/dt)\varphi_k^\xi(t) = h_k^{\text{MF}}(t)\varphi_k^\xi(t)$, where

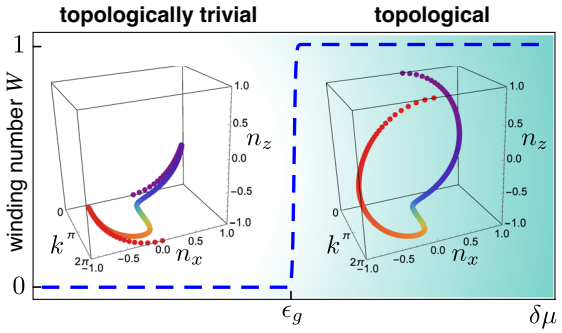

FIG. 1. Winding number W as a function of $\delta\mu$ (dashed line). In the inset we show the path of the vector $\vec{d}_k$ in the nontopological phase for $\delta\mu = 0.96 < \epsilon_g$ (left panel) and in the topological phase for $\delta\mu = 1.04 > \epsilon_g$. All energies are in units of ϵ_g and the function Δ_k is determined self-consistently for each $\delta\mu$.

$$h_k^{\text{MF}}(t) = \begin{pmatrix} -\epsilon_k & \Delta_k(t) \\ \Delta_k^*(t) & \epsilon_k \end{pmatrix} \quad (3)$$

is the physical mean-field Hamiltonian. The excitonic order parameter $\Delta_k(t) = \sum_q \tilde{U}_{k-q}\varphi^-_{cq}(t)\varphi^{-*}_{vq}(t)$ acquires a dependence on time through the wave functions. In Ref. [19] we have shown that this dependence is *monochromatic* and given by

$$\Delta_k(t) = \Delta_k e^{i\delta\mu t}. \quad (4)$$

Thus, the mean-field Hamiltonian supports self-sustained Josephson-like oscillations driven by the broken gauge symmetry. We then construct the Floquet Hamiltonian h_k^{Floq} from $\mathcal{T}e^{-i\int_0^T dt h_k^{\text{MF}}(t)} = e^{-ih_k^{\text{Floq}}T}$, where $\mathcal{T}$ is the time-ordered operator and $T = 2\pi/\delta\mu$, and look for nonvanishing Floquet topological invariants. Since $h_k^{\text{MF}}(t)$ is a 2×2 monochromatic and Hermitian matrix the Floquet Hamiltonian can easily be calculated [42]:

$$h_k^{\text{Floq}} = \begin{pmatrix} -\epsilon_k & \Delta_k \\ \Delta_k & \epsilon_k - \delta\mu \end{pmatrix} = -\frac{\delta\mu}{2}\mathbb{1} + e_k\vec{n}(k)\cdot\vec{\sigma}, \quad (5)$$

where $\sigma_{x,y,z}$ are the Pauli matrices and $\vec{n}(k) = \{n_x(k), n_y(k), n_z(k)\} = \{\Delta_k/e_k, 0, (\delta\mu/2 - \epsilon_k)/e_k\}$. Interestingly, h_k^{Floq} coincides with the NEQ gran-canonical mean-field Hamiltonian in Eq. (2) up to a constant diagonal shift. The winding number [43–45]

$$W = \frac{1}{2\pi}\int_{-\pi}^{\pi} d\Theta_k, \qquad \Theta_k = \arctan\frac{n_z(k)}{n_x(k)}, \quad (6)$$

measures the number of windings of the unit vector $\vec{d}_k = \{n_x(k), n_z(k)\}$ as k crosses the first Brillouin zone. W is a positive or negative integer in the topological phase and it is otherwise zero. It is immediate to realize that $W = 0$ for any

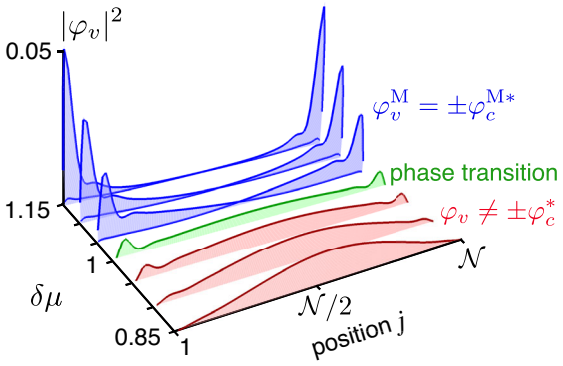

FIG. 2. Square modulus of the valence component of the eigenfunctions of the mean-field NEQ gran-canonical Hamiltonian with eigenvalue $e_{\rm max}$. For $\delta\mu < \epsilon_g$ the eigenvalue $e_{\rm max}$ is strictly negative and nondegenerate. For $\delta\mu > \epsilon_g$ the eigenvalue $e_{\rm max} = 0$ and the degeneracy is twofold. The corresponding eigenfunctions are Majorana modes. Energies are in units of ϵ_g.

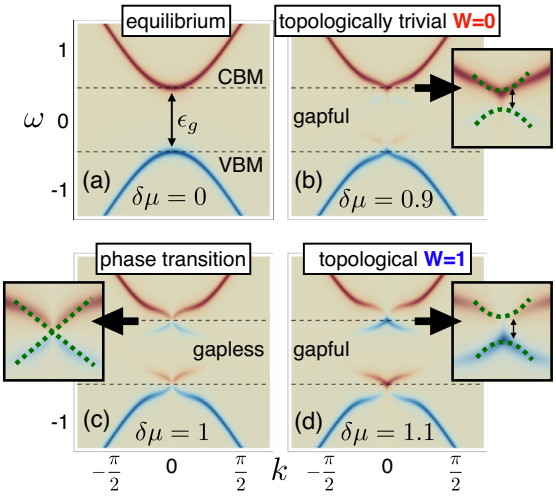

FIG. 3. Contour plot of the spectral function $A_k(\omega)$ for different values of $\delta\mu$. The red (blue) color refers to the removal contribution $A_k^<(\omega)$ [addition contribution $A_k^>(\omega)$]. The delta functions in Eq. (7) have been approximated by Lorentzians of width $\eta = 0.05$. The insets show a magnification of the spectral region around the conduction band minimum at $\epsilon_g/2$. All energies are in units of ϵ_g.

even Δ_k. If, instead, Δ_k is an odd function then $W = \pm 1$ provided that $\delta\mu > \epsilon_g$, see Fig. 1. Thus a topological transition occurs in a p-wave NEQ-EI as $\delta\mu$, and hence the electron density in the conduction band, exceeds a critical value. In Fig. 1 we also show the path of $\vec{d}_k$ resulting from the self-consistent solution of Eq. (2). The difference in chemical potentials is $\delta\mu = 0.96$ (left panel) and $\delta\mu = 1.04$ (right panel).

According to the bulk-edge correspondence, a number $|W|$ of topologically protected Floquet Majorana modes should form at each open boundary [44]. As the Floquet Hamiltonian in Eq. (5) coincides with the mean-field NEQ gran-canonical Hamiltonian in Eq. (2) we consider $\hat{H}_{\rm NEQ-GC}$ on an open wire of $\mathcal{N} = 100$ cells and solve the mean-field equations in the site basis. The spectrum is symmetric around zero energy with positive and negative eigenvalues $e_\lambda^+ = -e_\lambda^- \geq 0$. For $\delta\mu < \epsilon_g$ the maximum energy $e_{\rm max} = \max_\lambda\{e_\lambda^-\}$ is strictly negative and the eigenfunctions $\varphi_{\rm max}^\pm$ of energies $\pm e_{\rm max}$ are delocalized along the wire. In Fig. 2 we plot the valence probability $|\varphi_{{\rm max},vj}^+|^2$ versus site j (the conduction probability $|\varphi_{{\rm max},cj}^-|^2$ is identical). A sharp transition occurs for $\delta\mu > \epsilon_g$ since the spectrum is almost the same as for $\delta\mu < \epsilon_g$ except for two degenerate eigenvalues appearing at zero energy. The corresponding eigenfunctions can be chosen to satisfy $\varphi_{vj}^{\rm M} = \pm\varphi_{cj}^{\rm M^*}$, i.e., they are Majorana modes, and their valence components are plotted in Fig. 2. The Majorana modes are correctly localized at the system boundaries and the degree of localization increases as $\delta\mu$ moves deeper inside the topological phase.

The topological transition in a (bulk) p-wave NEQ-EI leaves unique fingerprints on the ARPES spectrum too. The spectral function $A_k(\omega)$ is the sum of a removal ($<$) and addition ($>$) contribution, $A_k(\omega) = A_k^<(\omega) + A_k^>(\omega)$ with

$$A_k^{\gtrless}(\omega) = |\varphi_{vk}^\pm|^2\delta\left(\omega \mp e_k + \frac{\delta\mu}{2}\right) + |\varphi_{ck}^\pm|^2\delta\left(\omega \mp e_k - \frac{\delta\mu}{2}\right). \tag{7}$$

In Fig. 3 we show how $A_k(\omega)$ changes from the equilibrium [panel (a)] to the symmetry-broken [panel (b)] and topological phase [panels (c)–(d)]. As $\delta\mu$ overcomes $\epsilon_x^p = 0.82$ the system becomes a nontopological NEQ-EI and an excitonic sideband appears inside the gap [panel (b)] [19,46]. For $\delta\mu = 0.9 < \epsilon_g$ the conduction density is $n_c = (1/\mathcal{N})\sum_k |\varphi_{ck}^-|^2 = 0.03$ and the averaged order parameter $\Delta \equiv (2/\mathcal{N})\sum_{0<k<\pi}\Delta_k = 0.04$ (with $\mathcal{N}$ the number of cells). The removal (blue) component of the excitonic structure is separated from the bottom of the conduction band (red) by a small gap, consistently with the insulating character of the state [inset of Fig. 3(b)]. In contrast with the s-wave NEQ-EI [19,47], however, the excitonic sideband has a vanishing spectral weight around the Γ point since $n_{ck} = |\varphi_{ck}^-|^2$ vanishes at $k = 0$ in the nontopological phase [see also the dashed line in Fig. 4(d)]. At the topological critical point ($\delta\mu = \epsilon_g = 1$) we find $n_c = 0.07$ and $\Delta = 0.06$ (both larger than for $\delta\mu = 0.9$). Despite $\Delta \neq 0$ the gap closes [inset of Fig. 3(c)] and the dispersion of the excitonic sideband around the Γ point becomes, see Eq. (7), $E_k \equiv (\delta\mu/2) - e_k \approx (\delta\mu/2) - \gamma|k|$ where we have approximated $\Delta_k \approx \gamma k$ [see also dashed lines in Fig. 4(c) and Fig. 5(c)]. Thus, the system becomes a Dirac semimetal. The transition point is also characterized by a discontinuity in $n_{ck=0}$ which varies abruptly from 0 ($\delta\mu < \epsilon_g$) to 1 ($\delta\mu > \epsilon_g$). In the topological phase $\delta\mu = 1.1 > \epsilon_g$ both $n_c = 0.11$ and

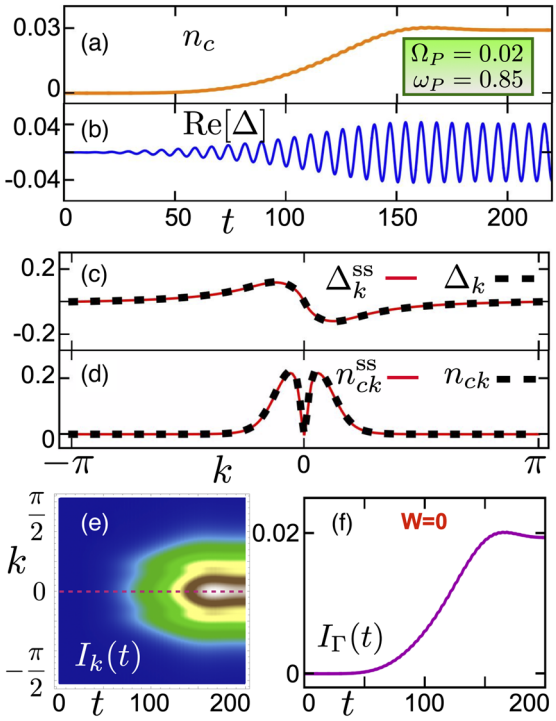

FIG. 4. Time evolution of the conduction density n_c [panel (a)] and the real part of the averaged order parameter Δ [panel (b)] induced by the laser pulse in Eq. (9) with $\Omega_P = 0.02$, $\omega_P = 0.85$, and $T_P = 200$. Comparison of Δ_k^{ss} and n_{ck}^{ss} [panels (c)–(d)] extracted from the real-time simulation (solid red lines) with the self-consistent Δ_k and n_{ck} obtained from Eq. (2) with $\delta\mu = \delta\mu^{ss} = 0.907$ (dashed black lines). Color plot of the time-resolved and momentum resolved intensity $I_k(t)$ defined in Eq. (10) [panel (e)] and its value $I_\Gamma(t)$ at the Γ-point [panel (f)]. Energies are in units of ϵ_g, and times in units of $1/\epsilon_g$.

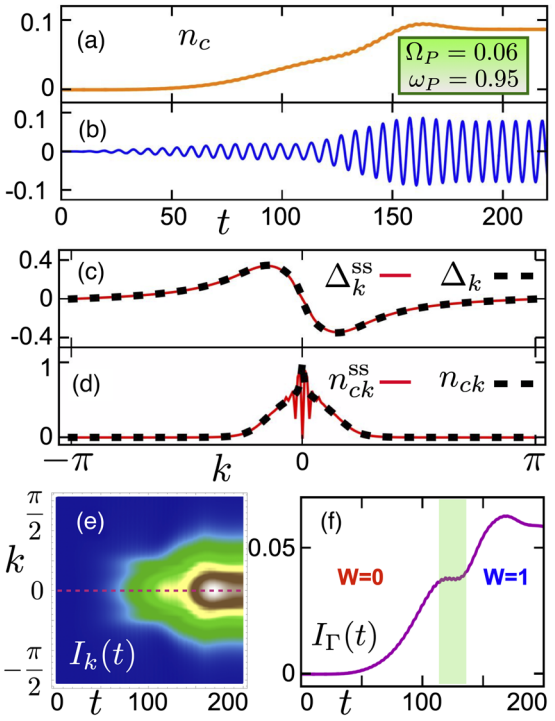

FIG. 5. Same as in Fig. 4 but with laser parameters $\Omega_P = 0.06$, $\omega_P = 0.95$, and $T_P = 200$. For the self-consistent solution of Eq. (2) we have used $\delta\mu = 1.04$. In panel (d) the green-shaded area separates the nontopological phase ($W = 0$) from the topological one ($W = 1$).

$\Delta = 0.08$ increase and the gap reopens, as Fig. 3(d) shows. Noteworthy, the spectral weight of the excitonic sideband is now largest at the Γ point due to the aforementioned discontinuity in $n_{ck=0}$.

The remaining issue to be addressed is whether and how the topological p-wave NEQ-EI state can be prepared. We answer affirmatively provided that the p-exciton is much brighter than the s exciton. We consider the system initially in the BI ground state and drive it out of equilibrium by a laser pulse,

$$\hat{H}_{\text{laser}}(t) = E(t)\sum_k D_k(\hat{\psi}_{ck}^\dagger\hat{\psi}_{vk} + \hat{\psi}_{vk}^\dagger\hat{\psi}_{ck}), \qquad (8)$$

where D_k is the valence-conduction dipole moment. The electric field $E(t)$ is a pulse of finite duration T_P centered around frequency ω_P:

$$E(t) = \theta(1 - |1 - 2t/T_P|)E_P \sin^2\left(\frac{\pi t}{T_P}\right)\sin(\omega_P t). \qquad (9)$$

To enhance absorption by the p exciton we take D_k odd in k.

First we generate the p-wave NEQ-EI in the nontopological phase by tuning the central frequency ω_P in the range $(\epsilon_x^p, \epsilon_g)$. In Fig. 4 we show the outcome of a real-time mean-field simulation performed with the CHEERS code [48] using $D_k = D\sin(k)$ and optimal laser parameters $T_P = 200$, the Rabi frequency $\Omega_P \equiv E_P D = 0.02$ and $\omega_P = 0.85$ (times in units of $1/\epsilon_g$). To find these parameters we implemented the searching scheme described in Ref. [19]. At the end of the pulse the system has steady occupations n_{ck}^{ss} giving a density $n_c = 0.03$ [panel (a)] and an averaged order parameter oscillating in time as $\Delta(t) = \Delta^{ss}e^{i\delta\mu^{ss}t}$ with steady-state amplitude $\Delta^{ss} = 0.04$ and $\delta\mu^{ss} = 0.907$ [panel (b)]. This oscillatory behavior is actually found for each k, i.e., $\Delta_k(t) = \Delta_k^{ss}e^{i\delta\mu^{ss}t}$ (not shown). We mention that the self-sustained oscillations (persistent at the mean-field level) survive for long enough time when numerically exact propagation schemes are used [49]. In panels (c)–(d) we compare Δ_k and n_{ck} obtained from the self-consistent solution of Eq. (2) at $\delta\mu = \delta\mu^{ss} < \epsilon_g$ against Δ_k^{ss} and n_{ck}^{ss} obtained from the real-time simulation. The agreement is remarkably good, thereby proving that a dynamical phase transition from a BI to a nontopological p-wave NEQ-EI can be induced by properly choosing the laser pulse. In fact, the steady-state spectrum

calculated long after the end of the pump is essentially the same as the self-consistent spectrum in Fig. 3(b), in agreement with Ref. [47]. In panel (e) we study the development of the momentum-resolved intensity of the excitonic sideband, proportional to $n_{ck}(t)$ according to Eq. (7). To account for the finite experimental resolution we calculate

$$I_k(t) = \sum_{q=k-\sigma/2}^{k+\sigma/2} n_{cq}(t), \tag{10}$$

with $\sigma = 2\pi/10$ (smaller σ values do not affect the conclusions). The cut at $k = 0$ (dashed-purple line) is displayed in panel (f) and it shows that the intensity $I_\Gamma(t) \equiv I_{k=0}(t)$ grows steadily in time until the end of the pulse.

Less obvious is the possibility of driving the BI toward a topological p-wave NEQ-EI. The BI ground state has $W = 0$ and hence the system should experience a *dynamical* topological transition featuring a gap closure at the quantum critical point. According to the Kibble-Zurek mechanism [21,22] this introduces a diverging timescale preventing the realization of the topological target state with an external field of *finite duration* T_P [50,51]. In fact, topological defects are produced around the Γ point (gap-closure point) for any $T_P < \infty$ [23–28]. One can easily prove that for odd dipoles D_k the density $n_{ck=0}(t) = 0$ at every time (in the topological phase $n_{ck=0} = 1$). In Fig. 5 we show the conduction density [panel (a)] and the averaged order parameter [panel (b)] for a laser pulse with $T_P = 200$, $\Omega_P = 0.06$, and $\omega_P = 0.95$. After the pulse ($t > T_P$) $n_c(t)$ attains a steady value and the averaged order parameter oscillates monochromatically as $\Delta(t) = \Delta^{\rm ss} e^{i\delta\mu^{\rm ss} t}$ with $\delta\mu^{\rm ss} = 1.04 > \epsilon_g$. As panel (c) shows, $\Delta_k^{\rm ss}$ is indistinguishable from the self-consistent Δ_k of Eq. (2) at $\delta\mu = \delta\mu^{\rm ss}$. We conclude that for $t > T_P$ the mean-field Hamiltonian has the same form as Eqs. (3), (4), and hence that the NEQ-EI is topological—the winding number W depends only on Δ_k, see Eq. (6). Although the two Hamiltonians are identical $n_{ck}^{\rm ss}$ differs from the self-consistent n_{ck} close to $k = 0$ [panel (d)], in agreement with the Kibble-Zurek mechanism. This topological defect, however, yields only a minor difference (around $k = 0$) between the self-consistent spectra [bottom panels of Fig. 3] and the steady-state spectra, again in agreement with Ref. [47].

In addition to the steady-state ARPES features discussed in Fig. 3, the topological transition produces a striking signature in the transient spectrum too. The time-dependent intensity of the excitonic sideband $I_k(t)$ [panel (e)] and in particular its value at the Γ point [panel (f)] exhibit a *plateau* (green-shaded area) just before the transition, estimated around $t \simeq 140$ [52]. Thus, the formation of topological defects hamper, according to Eq. (10), the occupation at Γ until the transition occurs, a phenomenon which we call "topological blockade." This blockade, absent in Fig. 4, lasts for 10%–20% of the pump duration and hence its observation should be within reach of modern time-resolved ARPES techniques [53].

To summarize, we have shown the existence of a Floquet topological phase in *nondriven* nonequilibrium matter and how to steer a nontopological BI toward this phase with laser pulses of finite duration. The nontrivial topology emerges exclusively from the electron-hole Coulomb attraction and it leaves unique fingerprints in time-resolved ARPES spectra. We observe that the inclusion of a finite exciton lifetime τ would damp the oscillations of the order parameter. However, as long as $\tau \gg (1/\epsilon_g)$ the excitonic spectral features highlighted in this work could still be observed. Experiments in this direction have already been performed in bulk transition metal dichalcogenides [54–56] having τ in the picosecond to nanosecond range [57–59] and $\epsilon_g \sim 1$–2 eV. Our discussion is based on a paradigmatic 1D model, but the results are general and can easily be extended to 2D systems. In this case the $p_x + ip_y$ symmetry of the EC order parameter can be exploited to generate a nonvanishing Chern number $(1/4\pi)\int d^2k\vec{n}\cdot(\partial_{k_x}\vec{n}\times\partial_{k_y}\vec{n})$ that, again, counts the Majorana edge modes. Materials with optically bright p excitons for realizing the topological p-wave NEQ-EI phase include semiconducting armchair nanotubes, in which only odd symmetry states are optically active when light is polarized along the tube axis [60–62], biased graphene bilayers [63], having them a $2p$ state with an oscillator strength about 20 times larger than that of the $1s$ state [64,65], semihydrogenated graphene [66], and low-dimensional compounds with strong spin-orbit coupling [67]. An s-wave NEQ-EI phase has been recently observed in bulk GaAs [68]: the way to light-induced topological phases of NEQ-EI is therefore already open.

We acknowledge useful discussions with Andrea Marini and Davide Sangalli. We also acknowledge funding from MIUR PRIN Grant No. 20173B72NB and from INFN17-Nemesys project.

[1] N. Read and D. Green, Phys. Rev. B **61**, 10267 (2000).
[2] M. Z. Hasan and C. L. Kane, Rev. Mod. Phys. **82**, 3045 (2010).
[3] X.-L. Qi and S.-C. Zhang, Rev. Mod. Phys. **83**, 1057 (2011).
[4] H. Hübener, U. De Giovannini, and A. Rubio, Nano Lett. **18**, 1535 (2018).
[5] M. C. Rechtsman, J. M. Zeuner, Y. Plotnik, Y. Lumer, D. Podolsky, F. Dreisow, S. Nolte, M. Segev, and A. Szameit, Nature (London) **496**, 196 (2013).
[6] J. Cayssol, B. Dóra, F. Simon, and R. Moessner, Phys. Status Solidi RRL **7**, 101 (2013).
[7] T. Kitagawa, E. Berg, M. Rudner, and E. Demler, Phys. Rev. B **82**, 235114 (2010).

[8] M. S. Rudner, N. H. Lindner, E. Berg, and M. Levin, Phys. Rev. X **3**, 031005 (2013).
[9] T. Östreich and K. Schönhammer, Z. Phys. B **91**, 189 (1993).
[10] C. Triola, A. Pertsova, R. S. Markiewicz, and A. V. Balatsky, Phys. Rev. B **95**, 205410 (2017).
[11] A. Pertsova and A. V. Balatsky, Phys. Rev. B **97**, 075109 (2018).
[12] R. Hanai, P. B. Littlewood, and Y. Ohashi, J. Low Temp. Phys. **183**, 127 (2016).
[13] R. Hanai, P. B. Littlewood, and Y. Ohashi, Phys. Rev. B **96**, 125206 (2017).
[14] R. Hanai, P. B. Littlewood, and Y. Ohashi, Phys. Rev. B **97**, 245302 (2018).
[15] K. W. Becker, H. Fehske, and V.-N. Phan, Phys. Rev. B **99**, 035304 (2019).
[16] M. Yamaguchi, K. Kamide, T. Ogawa, and Y. Yamamoto, New J. Phys. **14**, 065001 (2012).
[17] M. Yamaguchi, K. Kamide, R. Nii, T. Ogawa, and Y. Yamamoto, Phys. Rev. Lett. **111**, 026404 (2013).
[18] K. Hannewald, S. Glutsch, and F. Bechstedt, J. Phys. Condensed Matter **13**, 275 (2000).
[19] E. Perfetto, D. Sangalli, A. Marini, and G. Stefanucci, Phys. Rev. Mater. **3**, 124601 (2019).
[20] L. Jiang, T. Kitagawa, J. Alicea, A. R. Akhmerov, D. Pekker, G. Refael, J. I. Cirac, E. Demler, M. D. Lukin, and P. Zoller, Phys. Rev. Lett. **106**, 220402 (2011).
[21] T. W. B. Kibble, J. Phys. A **9**, 1387 (1976).
[22] W. H. Zurek, Nature (London) **317**, 505 (1985).
[23] K. Sengupta, D. Sen, and S. Mondal, Phys. Rev. Lett. **100**, 077204 (2008).
[24] S. Mondal, D. Sen, and K. Sengupta, Phys. Rev. B **78**, 045101 (2008).
[25] A. Bermudez, D. Patanè, L. Amico, and M. A. Martin-Delgado, Phys. Rev. Lett. **102**, 135702 (2009).
[26] A. Bermudez, L. Amico, and M. A. Martin-Delgado, New J. Phys. **12**, 055014 (2010).
[27] M. Lee, S. Han, and M.-S. Choi, Phys. Rev. B **92**, 035117 (2015).
[28] N. Defenu, G. Morigi, L. Dell'Anna, and T. Enss, Phys. Rev. B **100**, 184306 (2019).
[29] A. Y. Kitaev, Phys. Usp. **44**, 131 (2001).
[30] G. E. Volovik, J. Exp. Theor. Phys. Lett. **70**, 609 (1999).
[31] D. A. Ivanov, Phys. Rev. Lett. **86**, 268 (2001).
[32] C. Kallin and J. Berlinsky, Rep. Prog. Phys. **79**, 054502 (2016).
[33] M. Sato and Y. Ando, Rep. Prog. Phys. **80**, 076501 (2017).
[34] V. Gurarie and L. Radzihovsky, Ann. Phys. (Amsterdam) **322**, 2 (2007).
[35] L.-H. Hu, R.-X. Zhang, F.-C. Zhang, and C. Wu, arXiv:1912.09066.
[36] D. I. Pikulin and T. Hyart, Phys. Rev. Lett. **112**, 176403 (2014).
[37] L. Du, X. Li, W. Lou, G. Sullivan, K. Chang, J. Kono, and R.-R. Du, Nat. Commun. **8**, 1971 (2017).
[38] R. Wang, O. Erten, B. Wang, and D. Y. Xing, Nat. Commun. **10**, 210 (2019).
[39] M. S. Foster, V. Gurarie, M. Dzero, and E. A. Yuzbashyan, Phys. Rev. Lett. **113**, 076403 (2014).
[40] The mean-field Hamiltonian in Eq. (2) in principle contains a renormalization of the bare bands $\epsilon_{\alpha k}$ due to the Hartree self-energy. In this work we omit for simplicity such correction that, however, can be readsorbed in the defintion of the chemical potentials μ_α.
[41] D. Jérome, T. M. Rice, and W. Kohn, Phys. Rev. **158**, 462 (1967).
[42] E. Perfetto and G. Stefanucci, Phys. Rev. A **91**, 033416 (2015).
[43] Y. Niu, S. B. Chung, C.-H. Hsu, I. Mandal, S. Raghu, and S. Chakravarty, Phys. Rev. B **85**, 035110 (2012).
[44] Q.-J. Tong, J.-H. An, J. Gong, H.-G. Luo, and C. H. Oh, Phys. Rev. B **87**, 201109(R) (2013).
[45] M. Thakurathi, A. A. Patel, D. Sen, and A. Dutta, Phys. Rev. B **88**, 155133 (2013).
[46] E. Perfetto, D. Sangalli, A. Marini, and G. Stefanucci, Phys. Rev. B **94**, 245303 (2016).
[47] E. Perfetto, S. Bianchi, and G. Stefanucci, Phys. Rev. B **101**, 041201(R) (2020).
[48] E. Perfetto and G. Stefanucci, J. Phys. Condens. Matter **30**, 465901 (2018).
[49] Y. Murakami, M. Schüler, S. Takayoshi, and P. Werner, Phys. Rev. B **101**, 035203 (2020).
[50] E. Perfetto, Phys. Rev. Lett. **110**, 087001 (2013).
[51] P. D. Sacramento, Phys. Rev. E **90**, 032138 (2014).
[52] To locate the time of the topological transition we calculated the frequency $\omega_{\text{average}}(t)$ at which the running average of the Fourier transform of the order parameter [shown in Figure 5(b)] is peaked, and found that $\omega_{\text{average}}(t) = 1$ for $t = 136$. This is consistent with an independent evidence. At self-consistency $\delta\mu[n_c]$ is a monotonous increasing function of n_c. We have determined numerically this function, calculated $\delta\mu[n_c(t)]$ and found that $\delta\mu = 1$ for $t = 140$. Thus the plateau, located in time window (115,135), ends just before the topological transition.
[53] D. Kutnyakhov, R. P. Xian, M. Dendzik, M. Heber, F. Pressacco, S. Y. Agustsson, L. Wenthaus, H. Meyer, S. Gieschen, G. Mercurio *et al.*, Rev. Sci. Instrum. **91**, 013109 (2020).
[54] R. Bertoni, C. W. Nicholson, L. Waldecker, H. Hübener, C. Monney, U. De Giovannini, M. Puppin, M. Hoesch, E. Springate, R. T. Chapman *et al.*, Phys. Rev. Lett. **117**, 277201 (2016).
[55] M. Puppin, Freie Universität Berlin, Ph.d. thesis, 2018, http://dx.doi.org/10.17169/refubium-804.
[56] M. Puppin, Y. Deng, C. W. Nicholson, J. Feldl, N. B. M. Schrter, H. Vita, P. S. Kirchmann, C. Monney, L. Rettig, M. Wolf *et al.*, Rev. Sci. Instrum. **90**, 023104 (2019).
[57] H. Shi, R. Yan, S. Bertolazzi, J. Brivio, B. Gao, A. Kis, D. Jena, H. G. Xing, and L. Huang, ACS Nano **7**, 1072 (2013).
[58] Q. Cui, F. Ceballos, N. Kumar, and H. Zhao, ACS Nano **8**, 2970 (2014).
[59] M. Palummo, M. Bernardi, and J. C. Grossman, Nano Lett. **15**, 2794 (2015).
[60] S. Choi, J. Deslippe, R. B. Capaz, and S. G. Louie, Nano Lett. **13**, 54 (2013).
[61] E. Verdenhalven and E. Malić, J. Phys. Condens. Matter **25**, 245302 (2013).

[62] J. Maultzsch, R. Pomraenke, S. Reich, E. Chang, D. Prezzi, A. Ruini, E. Molinari, M. S. Strano, C. Thomsen, and C. Lienau, Phys. Rev. B **72**, 241402(R) (2005).
[63] C.-H. Park and S. G. Louie, Nano Lett. **10**, 426 (2010).
[64] T. Cao, M. Wu, and S. G. Louie, Phys. Rev. Lett. **120**, 087402 (2018).
[65] C.-H. Park and S. G. Louie, Nano Lett. **10**, 426 (2010).
[66] Z. Jiang, W. Lou, Y. Liu, Y. Li, H. Song, K. Chang, W. Duan, and S. Zhang, Phys. Rev. Lett. **124**, 166401 (2020).
[67] I. Garate and M. Franz, Phys. Rev. B **84**, 045403 (2011).
[68] Y. Murotani, C. Kim, H. Akiyama, L. N. Pfeiffer, K. W. West, and R. Shimano, Phys. Rev. Lett. **123**, 197401 (2019).